Supplementary Information for

Chemical waves in reaction-diffusion networks of small organic molecules

Arpita Paikar,[1#] Xiuxiu Li,[1,2#] Liat Avram,[3] Barbara S. Smith,[4] István Sütő,[5] Dezső Horváth,[6] Elisabeth Rennert,[7] Yuqing Qiu,[8] Ágota Tóth,[5] Suriyanarayanan Vaikuntanathan,[8] and Sergey N. Semenov[1*]

1. *Department of Molecular Chemistry and Materials Science, Weizmann Institute of Science, Rehovot, Israel*
2. *Department of Chemistry and Shenzhen Key Laboratory of Small Molecule Drug Discovery and Synthesis, Southern University of Science and Technology, Shenzhen, China*
3. *Department of Chemical Research Support, Weizmann Institute of Science, Rehovot, Israel*
4. *School of Biological and Health Systems Engineering, Arizona State University, Tempe, Arizona, United States*
5. *Department of Physical Chemistry and Materials Science, University of Szeged, Szeged, Hungary*
6. *Department of Applied and Environmental Chemistry, University of Szeged, Szeged, Hungary*
7. *Graduate Program in Biophysical Sciences, University of Chicago, Chicago, IL, United States*
8. *Department of Chemistry, University of Chicago, Chicago, IL, United States*

 # These authors contributed equally to this work

*Correspondence to: sergey.semenov@weizmann.ac.il

Table of Content

Materials and methods

Thiourea, (2-bromoethyl)trimethylammonium bromide, Cystamine dihydrochloride, Maleimide, Acrylamide, Agarose, N-methylcarbonylmaleimide, Sodium sulfate, Sodium bicarbonate, Sodium chloride, 5,5′-Disulfanediylbis(2-nitrobenzoic acid) (Ellman's reagent), Hydrochloric acid, Monopotassium phosphate, Dipotassium phosphate, Tris base, and Tris hydrochloride were purchased from Sigma Aldrich, Acros Organics, Alfa Aesar, and Merck. Solvents – Dichloromethane, Chloroform, Methanol, Ethanol, Hexane, Ethyl acetate, Acetone, anhydrous Tetrahydrofuran and Diethyl ether were purchased from Sigma-Aldrich and Acros Organics. D_2O was purchased form Tzamal d-chem; all other NMR solvents were purchased from Cambridge Isotope Laboratories. All chemicals, including solvents, were used without further purification.

NMR spectra were measured on a Bruker AVANCE III-300 spectrometer at 300 MHz for ^{1}H and 73.7 MHz for $^{13}C\{1H\}$, on a Bruker AVANCE NEO 400 spectrometer at 400 MHz for ^{1}H and 100.6 MHz for $^{13}C\{1H\}$, and on a Bruker AVANCE III HD-500 spectrometer at 500 MHz for ^{1}H and 125.8 MHz for $^{13}C\{1H\}$. Chemical shifts for ^{1}H and ^{13}C are given in ppm relative to TMS. ^{1}H and ^{13}C spectra were calibrated using a residual solvent peak as an internal reference (D_2O ^{1}H NMR: $\delta = 4.79$ ppm; $CDCl_3$ ^{1}H NMR: $\delta = 7.26$ ppm, ^{13}C NMR: $\delta = 77$ ppm). Data for the ^{1}H NMR spectra were reported as follows: chemical shift (ppm), peak shape (s = singlet, d = doublet, t = triplet, q = quartet, p = pentet, m = multiplet, br = broad, dd = doublet of doublets), coupling constant (Hz), and integration.

High-resolution mass spectra were recorded on a Waters Xevo G2- XS QTof mass spectrometer (Manchester, UK) with an electrospray ionization (ESI) source.

The reactants in the flow experiments were supplied by NEMESYS Low Pressure Syringe pumps (Gear: 14:1, Type: NEM-B101-02E), produced by CETONI GmbH.

Synthesis

We synthesized thiouronim salt **(1)**,[1] and thiol sensor[2] following the published protocols**.** To obtain PEG-maleimides, we used a modified literature protocol (Fig. S1).[3]

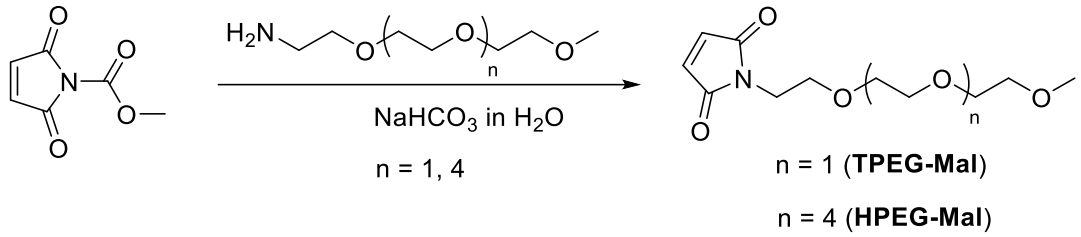

Figure S1. General scheme of synthesis for PEG-Maleimides.

Synthesis of HPEG-Mal: A required amount of Me-Peg-6-NH_2 (267.4mg, 1.09 mmol) was dissolved in a saturated aqueous solution of $NaHCO_3$ (3.34 mmol) and the solution was stirred for 10 min in an ice bath. Then N-methylcarbonylmaleimide (169.1mg, 1.09 mmol) was added to the solution, and the reaction mixture was stirred at 0 °C for 20 min and in room temperature for another 20 min. Then, the reaction mixture was extracted with $CHCl_3$, washed with brine, and the organic layer was collected. It was dried over Na_2SO_4 and evaporated to dryness under vacuum to obtain an oily compound. The crude yield 360 mg (88%). Purity can be determined using an internal standard as the compound may contain water due to the long PEG tail. ^{1}H NMR of HPEG-Mal (400 MHz, $CDCl_3$, δ): 6.67 (2H, s, CH), 3.70-3.67 (2H, m -NCH_2), 3.63-3.50 (all -OCH_2CH_2, m, 20H), 3.70-3.67 (2H, m, -OCH_2), 3.34 (3H, s, -OMe). ^{13}C NMR: (100.6 MHz, $CDCl_3$, δ): 171.05, 134.55, 72.30, 70.98-70.87 (peg CH_2), 70.42, 68.19. HRMS (ESI) m/z: [M+Na]+ calcd. for $C_{17}H_{29}NNaO_8^+$: 398.1785; found 398.1770.

Synthesis of TPEG-Mal: We used the same procedure as for HPEG-Mal. Here, Me-Peg-3-NH_2 (177.9mg, 1.09 mmol) was taken, and the rest of the reagents were used in the same amounts. Crude yield 244 mg, 92%. Purity can be determined using an internal standard as the compound may contain water due to the long PEG tail. ^{1}H NMR of TPEG-Mal (400 MHz, $CDCl_3$, δ): 6.69 (2H, s, CH), 3.73-3.70 (2H, m -NCH_2,), 3.65-3.59 (all -OCH_2CH_2, m, 8H), 3.53-3.51 (2H, m, -OCH_2), 3.36 (3H, s, -OMe). ^{13}C NMR (100.6 MHz, $CDCl_3$): 171.12, 134.61, 72.39, 71.03, 70.53, 68.30, 59.50, 37.61. HRMS (ESI) m/z: [M+Na]+ calcd. for $C_{11}H_{17}NNaO_5^+$: 266.1004; found 266.1009.

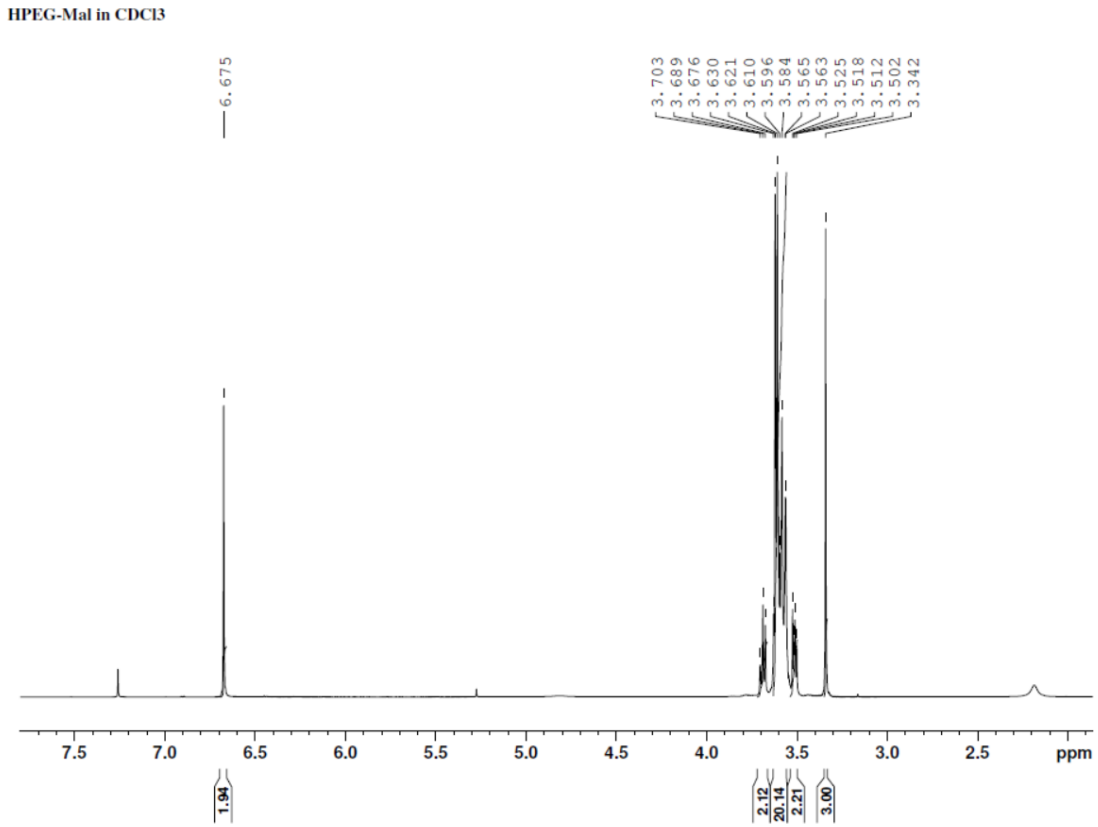

Figure S2. [1]H NMR of HPEG-Mal

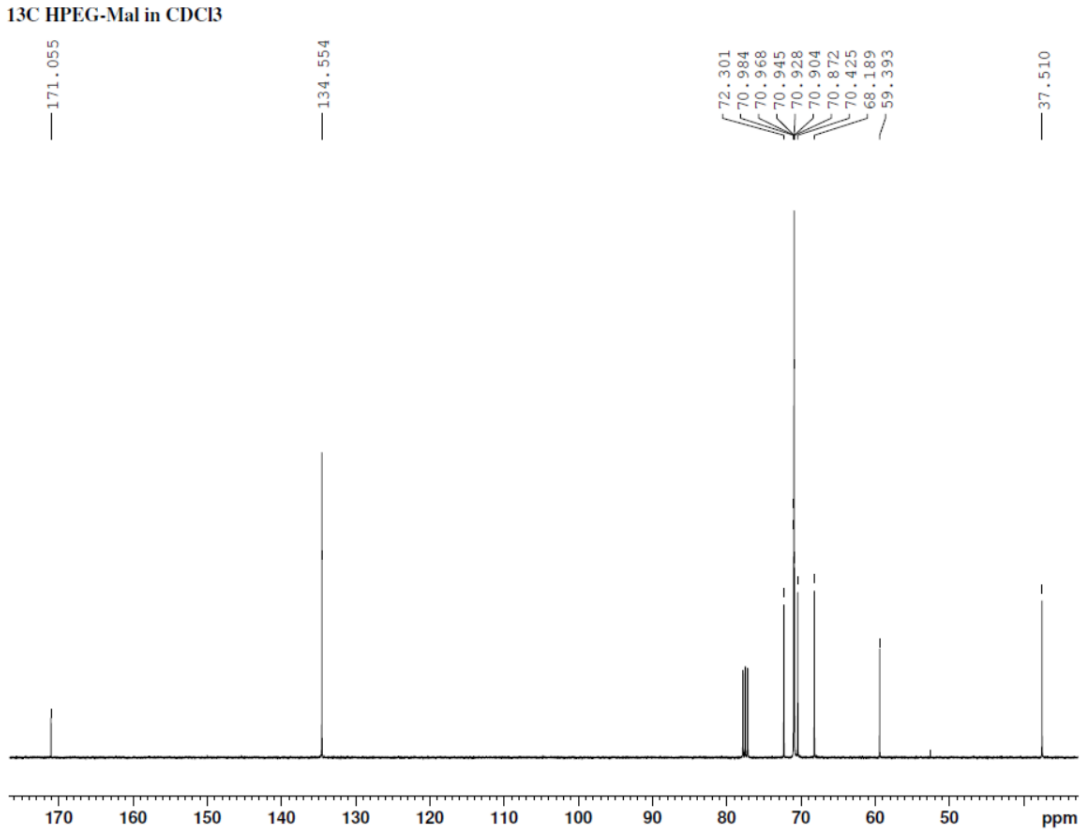

Figure S3. [13]C NMR of HPEG-Mal

Figure S4. HRMS of HPEG-Mal

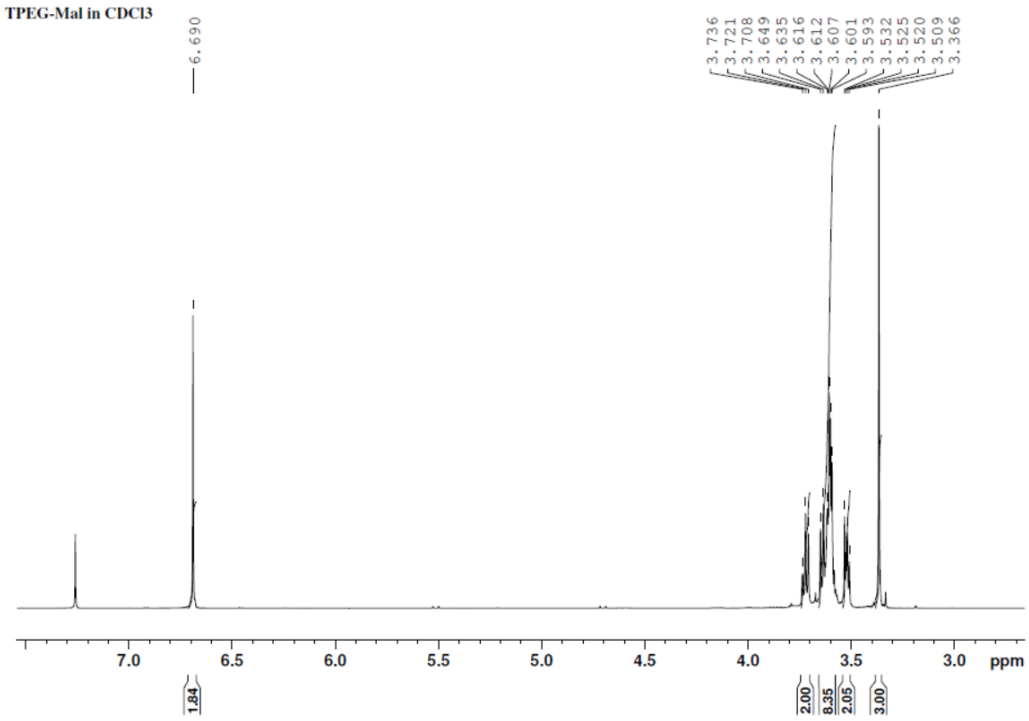

Figure S5. ^{1}H NMR of TPEG-Mal

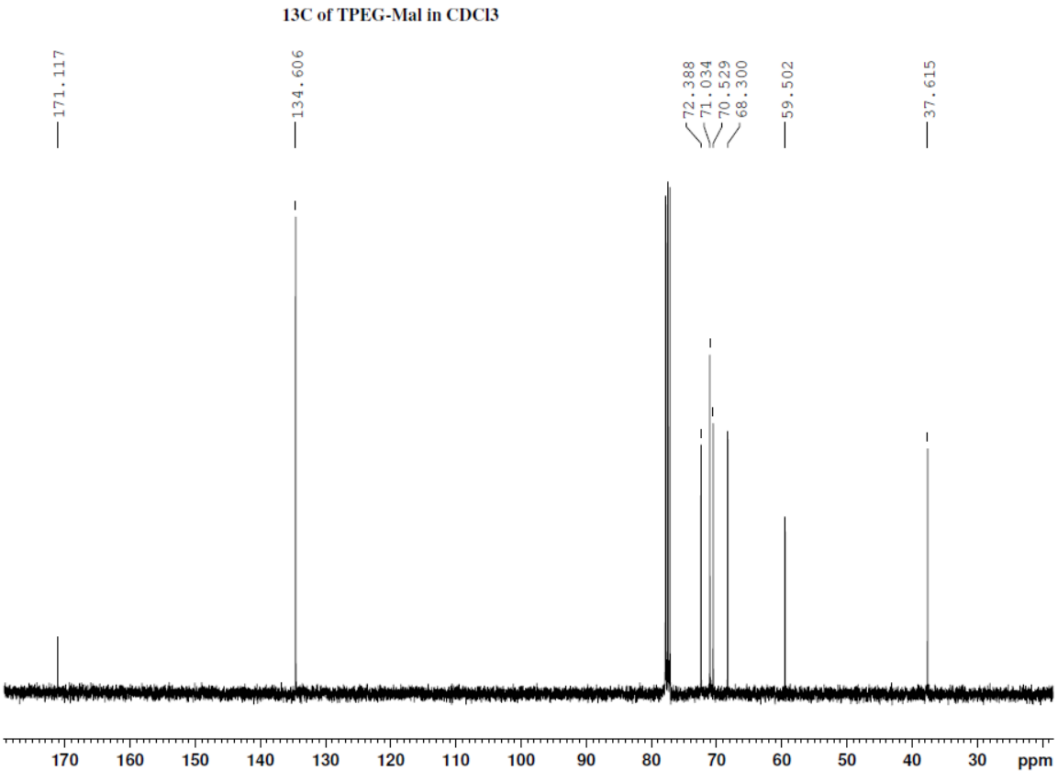

Figure S6. ^{13}C NMR of TPEG-Mal

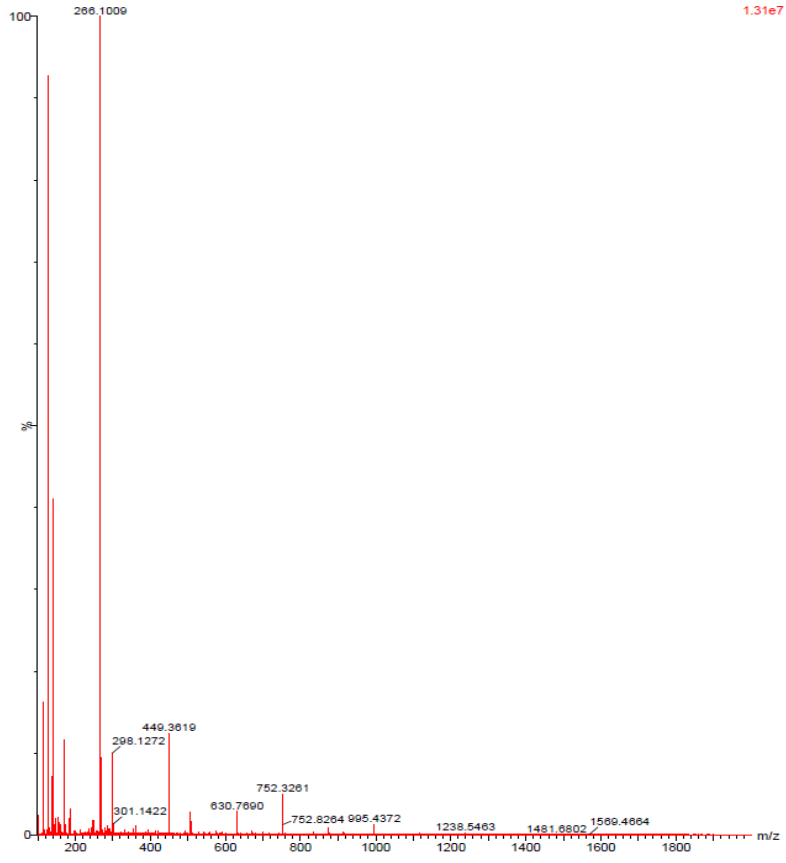

Figure S7. HRMS of TPEG-Mal

Flow experiments

(I) Construction of the reactor

We took a rectangular brass block (10x5x2 mm, size varies according to our experimental needs) with two channels (0.9 mm diameter) inside the block (Fig. S8a). This block was placed inside a Petri dish, and four holes were made in the Petri dish to insert two 0.9 mm needles through the channels of the brass block (Fig. S8b). The block was positioned in the middle of the Petri dish, which was then filled with a mixture of degassed Sylgard® 184 silicone elastomer with 9 wt% of the curing agent on top of the brass block, ensuring that the polymer covered the flat surface of the brass block. A smaller Petri dish was placed flat side down on top of the brass block surface to flatten the surface and to ensure that, after curing, the solid PDMS mold would have a height of 2 mm. The entire assembly was then placed in an oven at 80°C for about 2 hours for curing. After removing it from the oven, we removed the needles and cut the solid PDMS, keeping the block in the middle. The PDMS layer was then removed from the Petri dish, and the block was taken out, forming a rectangular cavity in the PDMS layer with the dimensions of the brass block. Next, one side of the PDMS layer was plasma-bonded to a glass slide.[4] The resulting structure was used as the reactor for the flow experiments (Fig. S8c).

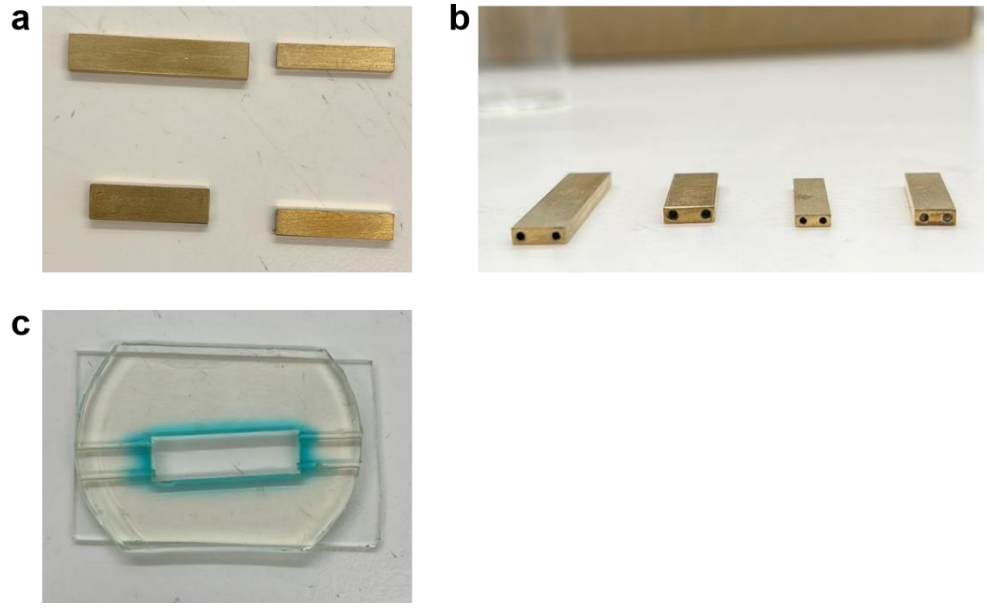

Figure S8. a) Top view of different brass blocks. b) Front view of different brass blocks with holes. c) Reactor with two channels made from PDMS.

(II) Assembling components

Our flow setup can be divided into four main components: (i) syringe pumps, (ii) a reactor with two channels and an agarose gel bed, (iii) a microfluidic pre-mixer (or two mixers), and (iv) a camera.

(i) Syringe pumps: We used NEMESYS Low Pressure Syringe pumps from CETONI in all our experiments. The construction of the two-channel reactor and microfluidic mixers is described in detail below.

(ii) Reactor with Agarose hydrogel: We took the PDMS reactor and inserted two 0.9 mm needles into the channels. Then, we poured a hot 1% agarose solution to fill the reactor cavity and placed a glass slide on top of it. The assembly was left to cool down and solidify for a few minutes. Next, we carefully removed the two needles to avoid breaking the solid agarose gel, thus forming two smooth channels inside the hydrogel. Finally, we secured the reactor with the glass slide on top using two metal paper clips on either side (Fig. S9).

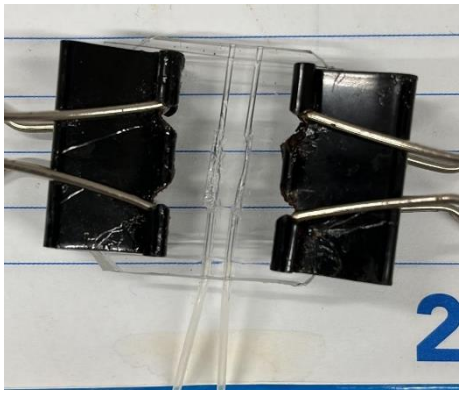

Figure S9. Assembled reactor with agarose hydrogel inside and top glass fixed by metal clips.

(iii) Microfluidic mixers: We used either commercially available microfluidic T-shaped pre-mixers or self-made microfluidic pre-mixers from PDMS. The protocol for preparing the self-made pre-mixers is as follows. We took three hypodermic needles (diameter 0.9 mm), cut them to ~1 cm length, and placed them in a 5 cm plastic Petri dish such that the ends of two needles touched each other, and the end of the third needle was ~1 cm from the junction. Next, we filled the Petri dish with a mixture of Sylgard® 184 silicone elastomer with 9 wt% of the curing agent. The mixture was degassed under reduced pressure and cured for 2 hours at 80 °C to form a solid polydimethylsiloxane (PDMS) elastomer. After curing, the needles were removed, and the PDMS was taken out of the Petri dish. The channel between the junction and the third inlet was manually scratched, and the device was plasma bonded to a microscope glass slide.

(iv) Camera: We used a USB camera (model Logitech C920) positioned above the reactor to monitor changes in the hydrogel throughout the experiments. We captured pictures of the reactor every 1 minute

until the flow stopped (approximately 8-10 hours for all the experiments). The pictures were then transferred and compiled into a time-lapse video using CyberLink PowerDirector 18 software.

(III) Running flow

(i) Preparing solutions. We prepared solutions for the syringes, with the composition varying according to the experiments. We used setups with either 3 or 4 syringes. In the 3-syringe setup, **Mal** was used in only one syringe due to its high diffusion coefficient, allowing it to fill the entire hydrogel by diffusing from one side. In the 4-syringe setup, **Mal**, **TPEG-Mal**, or **HPEG-Mal** were supplied from two syringes, enabling the maleimide derivatives to diffuse into the hydrogel from both sides. This condition allows for faster filling of the hydrogel with maleimide derivatives, which is critical for the slow-diffusing **TPEG-Mal** and **HPEG-Mal**.

3-Syringe setup:

Syringe 1: **1** (96.9 mg), **Mal** (2.18 mg), **3** (170.59 mg), and **Thiol sensor** were dissolved in 1.5 mL of HPLC water. Resulting concentrations of reactants were: **1** (200 mM), **Mal** (15 mM), **3** (1600 mM).

Syringe 2: 2M Tris pH 7.5 1.5 mL.

Syringe 3: 2 (135.12 mg) and **Thiol sensor** were dissolved in 3 mL of 1M Tris pH 7.5. Resulting concentration of **2** was 200mM.

4-Syringe setup:

Syringe 1: **1** (96.9 mg), the required amount of **Mal**, **TPEG-Mal,** or **HPEG-Mal** (depending on the particular experiment), **3** (170.59 mg), and **Thiol sensor** were dissolved in 1.5 mL of HPLC water. Resulting concentrations of reactants were: **1** (200 mM), **Mal**, **TPEG-Mal,** or **HPEG-Mal** (depending on the experiment), **3** (1600 mM).

Syringe 2: 2M Tris pH 7.5 1.5 mL.

Syringe 3: 2 (135.12 mg) and **Thiol sensor** were dissolved in 3 mL of 1M Tris pH 7.5. Resulting concentration of **2** was 200mM..

Syringe 4: Required amount of **Mal**, **TPEG-Mal,** or **HPEG-Mal** (depending on the experiment) and **Thiol sensor** were dissolved in 1.5 mL of 1M Tris pH 7.5.

(ii) Connecting components. Next, we connected all the components. The syringes were connected with PTFE tubing (0.7 mm inner diameter) using three hypodermic needles (0.85 mm diameter). In 3-synge setup, the tubes from syringes 1 and 2 were connected to the two inlets of the mixer. One tube connected the outlet of the mixer to one of the inlet channels of the reactor. Then, the tubing from the 3rd syringe was connected to the 2nd inlet channel of the reactor. We also connected two small tubings to the outlets of the reactor and placed a Petri dish at the end of these tubings to collect waste (Fig. S10).

In 4-synge setup, we used two mixers. Syringes 1 and 2 were connected to the first mixer, while syringes 3 and 4 were connected to the second mixer. The outlets of the mixers were connected to the inlet channels of the reactor.

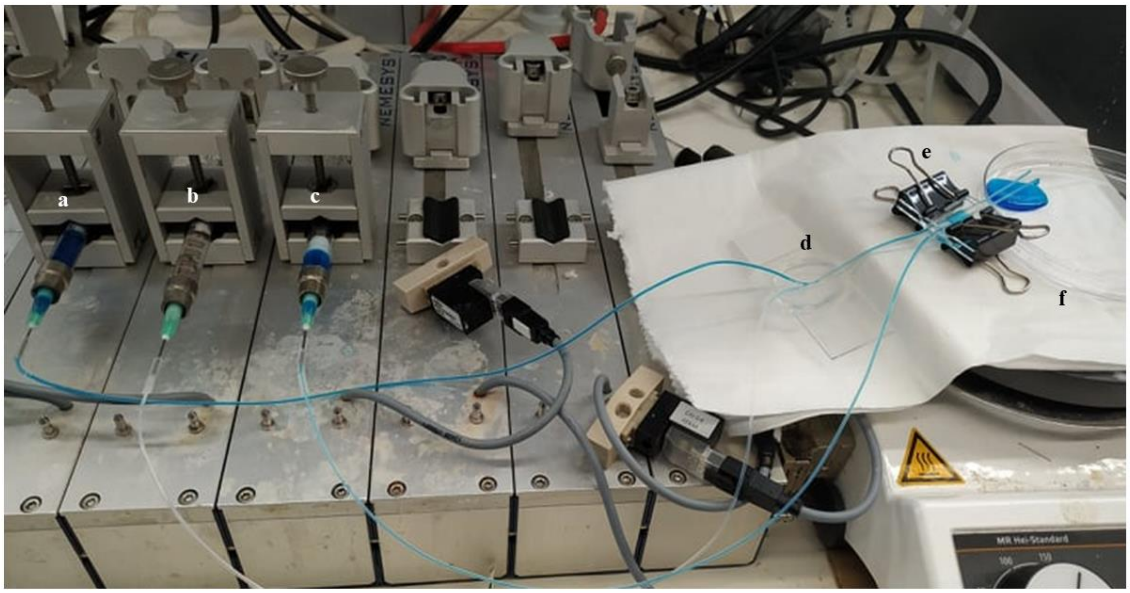

Figure S10. The complete setup for the flow experiments. **a**, **b**, and **c** Three syringes with reagents. **d** Pre-mixer connected with reactor via two channels. **e** PDMS reactor with agarose gel. **f** Petri dish for collecting waste.

(iii) Flowing reagents and collecting images. Next, we filled the tubing by pumping solutions at a flow rate of 3000 µl/hour in each channel to fill the tubes and check for leakages. In the 3-syringe setup, flows from the first and second syringes were equal, while the third syringe had double the flow rate to ensure equal flow in the channels of the hydrogel. In the 4-syringe setup, flows from all syringes were equal. Then, we reduced the flow rates in each channel to the required value (usually between 200 and 400 µl/hour, equal in both channels of the hydrogel) and ran the experiment for the next 6-12 hours. During the experiments, we acquired images of the reactor every minute. Later, these images were assembled into videos.

Summary of the conditions for flow experiments

Experimental parameters for all flow experiments are summarized in Table S1. The second code represents a number for the corresponding video.

Code	Reactor Size(mm)	Concentration in the channel	Flow rate (µl/hr)	Result
Exp1 Vid1	5x20x2	Channel 1: [**1**] = 100 mM, [**Mal**] = 10 mM, [**3**] = 800 mM; Channel 2: [**2**] = 200 mM	200/200	Very distinctive consecutive wave forms
Exp2 Vid2	7x20x2	Channel 1: [**1**] = 100 mM, [**Mal**] = 10 mM, [**3**] = 800 mM; Channel 2: [**2**] = 200 mM	200/200	Wave from both the side, looks like cell division
Exp3 Vid3	5x30x2	Channel 1: [**1**] = 100 mM, [**Mal**] = 10 mM, [**3**] = 800 mM; Channel 2: [**2**] = 200 mM	200/200	Very distinctive consecutive wave forms, 2 even 3 also forms in one gel
Exp4	5x20x2	Channel 1: [**1**] = 100 mM, [**Mal**] = 10 mM, [**3**] = 800 mM; Channel 2: [**2**] = 200 mM	300/300	Seven waves
Exp5 Vid4	5x20x2	Channel 1: [**1**] = 100 mM, [**Mal**] = 8 mM, [**3**] = 800 mM; Channel 2: [**2**] = 200 mM, [**Mal**] = 4 mM	300/300	Eight waves
Exp6 Vid5	5x20x2	Channel 1: [**1**] = 100 mM, [**Mal**] = 10 mM, [**3**] = 800 mM; Channel 2: [**2**] = 200 mM, [**Mal**] = 4 mM	300/300	Six waves, propagation looks good
Exp7 Vid6	5x20x2	Channel 1: [**1**] = 100 mM, [**Mal**] = 11 mM, [**3**] = 800 mM; Channel 2: [**2**] = 200 mM, [**Mal**] = 5 mM	300/300	Five waves, propagation looks good
Exp8 Vid7	5x20x2	Channel 1: [**1**] = 100 mM, [**Mal**] = 13.5 mM, [**3**] = 800 mM; Channel 2: [**2**] = 200 mM, [**Mal**] = 6.5 mM	300/300	Three waves
Exp9 Vid8	5x20x2	Channel 1: [**1**] = 100 mM, [**Mal**] = 16 mM, [**3**] = 800 mM; Channel 2: [**2**] = 200 mM, [**Mal**] = 8 mM	300/300	Only one ending wave
Exp10	7x20x2	Channel 1: [**1**] = 100 mM, [**TPEG-Mal**] = 8 mM, [**3**] = 800 mM; Channel 2: [**2**] = 200 mM, [**TPEG-Mal**] = 3 mM	200/200	Initially one wave

Exp11	7x20x2	Channel 1: [**1**] = 100 mM, [**TPEG-Mal**] = 7 mM, [**3**] = 800 mM; Channel 2: [**2**] = 200 mM, [**TPEG-Mal**] = 3 mM	200/200	Initially one wave, formed from Channel 1 side
Exp12	5x20x2	Channel 1: [**1**] = 100 mM, [**TPEG-Mal**] = 8 mM, [**3**] = 800 mM; Channel 2: [**2**] = 200 mM, [**TPEG-Mal**] = 3 mM	200/200	Initially one wave
Exp13	5x20x2	Channel 1: [**1**] = 100 mM, [**TPEG-Mal**] = 7 mM, [**3**] = 800 mM; Channel 2: [**2**] = 200 mM, [**TPEG-Mal**] = 2 mM	300/300	Initially one wave
Exp14	5x20x2	Channel 1: [**1**] = 100 mM, [**TPEG-Mal**] = 10 mM, [**3**] = 800 mM; Channel 2: [**2**] = 200 mM, [**TPEG-Mal**] = 4 mM	300/300	Three waves, the third one is very faint
Exp15	5x20x2	Channel 1: [**1**] = 100 mM, [**TPEG-Mal**] = 14 mM, [**3**] = 800 mM; Channel 2: [**2**] = 200 mM, [**TPEG-Mal**] = 6 mM	300/300	Four waves, the third one and fourth one are faint
Exp16	5x20x2	Channel 1: [**1**] = 100 mM, [**TPEG-Mal**] = 16 mM, [**3**] = 800 mM; Channel 2: [**2**] = 200 mM, [**TPEG-Mal**] = 8 mM	300/300	Five waves
Exp17	5x20x2	Channel 1: [**1**] = 100 mM, [**TPEG-Mal**] = 16 mM, [**3**] = 800 mM; Channel 2: [**2**] = 200 mM, [**TPEG-Mal**] = 8 mM	400/400	Six waves
Exp18	5x20x2	Channel 1: [**1**] = 100 mM, [**TPEG-Mal**] = 16 mM, [**3**] = 800 mM; Channel 2: [**2**] = 200 mM, [**TPEG-Mal**] = 8 mM	200/200	Four waves
Exp19	5x20x2	Channel 1: [**1**] = 100 mM, [**TPEG-Mal**] = 18.7 mM, [**3**] = 800 mM; Channel 2: [**2**] = 200 mM, [**TPEG-Mal**] = 9.3 mM	300/300	Only two traveling waves, propagation looks very good
Exp20	5x20x2	Channel 1: [**1**] = 100 mM, [**TPEG-Mal**] = 18.7 mM, [**3**] = 800 mM;	300/300	Three traveling waves

		Channel 2: [**2**] = 200 mM, [**TPEG-Mal**] = 9.3 mM		
Exp21	5x20x2	Channel 1: [**1**] = 100 mM, [**TPEG-Mal**] = 20 mM, [**3**] = 800 mM; Channel 2: [**2**] = 200 mM, [**TPEG-Mal**] = 10 mM	300/300	Five traveling waves
Exp22	5x20x2	Channel 1: [**1**] = 100 mM, [**TPEG-Mal**] = 22.7 mM, [**3**] = 800 mM; Channel 2: [**2**] = 200 mM, [**TPEG-Mal**] = 11.3 mM	300/300	Three traveling waves (reaction time is short (6 h), then tried to extend the reaction time to 12 h in xiu-269)
Exp23	5x20x2	Channel 1: [**1**] = 100 mM, [**TPEG-Mal**] = 22.7 mM, [**3**] = 800 mM; Channel 2: [**2**] = 200 mM, [**TPEG-Mal**] = 11.3 mM	300/300	Six waves, propagation looks good
Exp24	5x20x2	Channel 1: [**1**] = 100 mM, [**TPEG-Mal**] = 22.7 mM, [**3**] = 800 mM; Channel 2: [**2**] = 200 mM, [**TPEG-Mal**] = 11.3 mM	300/300	Six waves, the fifth one and sixth one are faint (repeated reaction of xiu-269)
Exp25 Vid9	5x20x2	Channel 1: [**1**] = 100 mM, [**TPEG-Mal**] = 25.5 mM, [**3**] = 800 mM; Channel 2: [**2**] = 200 mM, [**TPEG-Mal**] = 12.5 mM	300/300	Five waves, propagation looks better
Exp26	5x20x2	Channel 1: [**1**] = 100 mM, [**HPEG-Mal**] = 5.4 mM, [**3**] = 800 mM; Channel 2: [**2**] = 200 mM, [**HPEG-Mal**] = 2.0 mM	200/200	Initially one faint wave
Exp27	5x20x2	Channel 1: [**1**] = 100 mM, [**HPEG-Mal**] = 8 mM, [**3**] = 800 mM; Channel 2: [**2**] = 200 mM, [**HPEG-Mal**] = 3 mM	300/300	Initially one distinct wave
Exp28	5x20x2	Channel 1: [**1**] = 100 mM, [**HPEG-Mal**] = 10 mM, [**3**] = 800 mM; Channel 2: [**2**] = 200 mM, [**HPEG-Mal**] = 4 mM	400/400	Initially one distinct wave
Exp29	5x20x2	Channel 1: [**1**] = 100 mM, [**HPEG-Mal**] = 24 mM, [**3**] = 800 mM; Channel 2: [**2**] = 200 mM, [**HPEG-Mal**] =	300/300	Three waves

		12 mM		
Exp30	5x20x2	Channel 1: [**1**] = 100 mM, [**HPEG-Mal**] = 30 mM, [**3**] = 800 mM; Channel 2: [**2**] = 200 mM, [**HPEG-Mal**] = 14 mM	300/300	Five waves, the fourth one and fifth one are faint
Exp31	5x20x2	Channel 1: [**1**] = 100 mM, [**HPEG-Mal**] = 32 mM, [**3**] = 800 mM; Channel 2: [**2**] = 200 mM, [**HPEG-Mal**] = 16 mM	300/300	Five waves
Exp32 Vid10	5x20x2	Channel 1: [**1**] = 100 mM, [**HPEG-Mal**] = 35 mM, [**3**] = 800 mM; Channel 2: [**2**] = 200 mM, [**HPEG-Mal**] = 17 mM	300/300	Four traveling waves, propagation looks good

Finding conditions for sustained waves

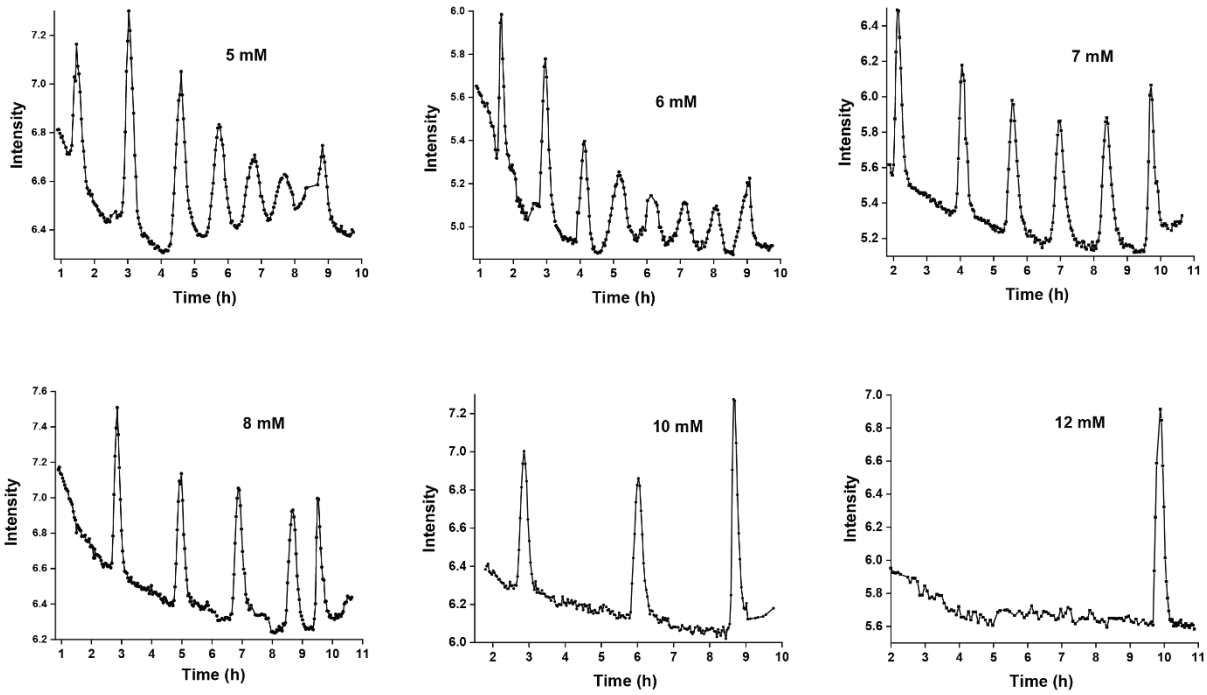

Figure S11. Oscillatory plots from experiments with different amounts of **Mal**. The plots were obtained by measuring intensity at a chosen point in the hydrogel (for details, see the data analysis section). The average **Mal** concentration between the two channels is shown in the plots. This number approximately reflects the concentration of **Mal** in the middle of the hydrogel after equilibration. Detailed experimental conditions for the experiments used in this figure can be found in **Table S1** under labels Exp4-9 (order is left to right, top to bottom).

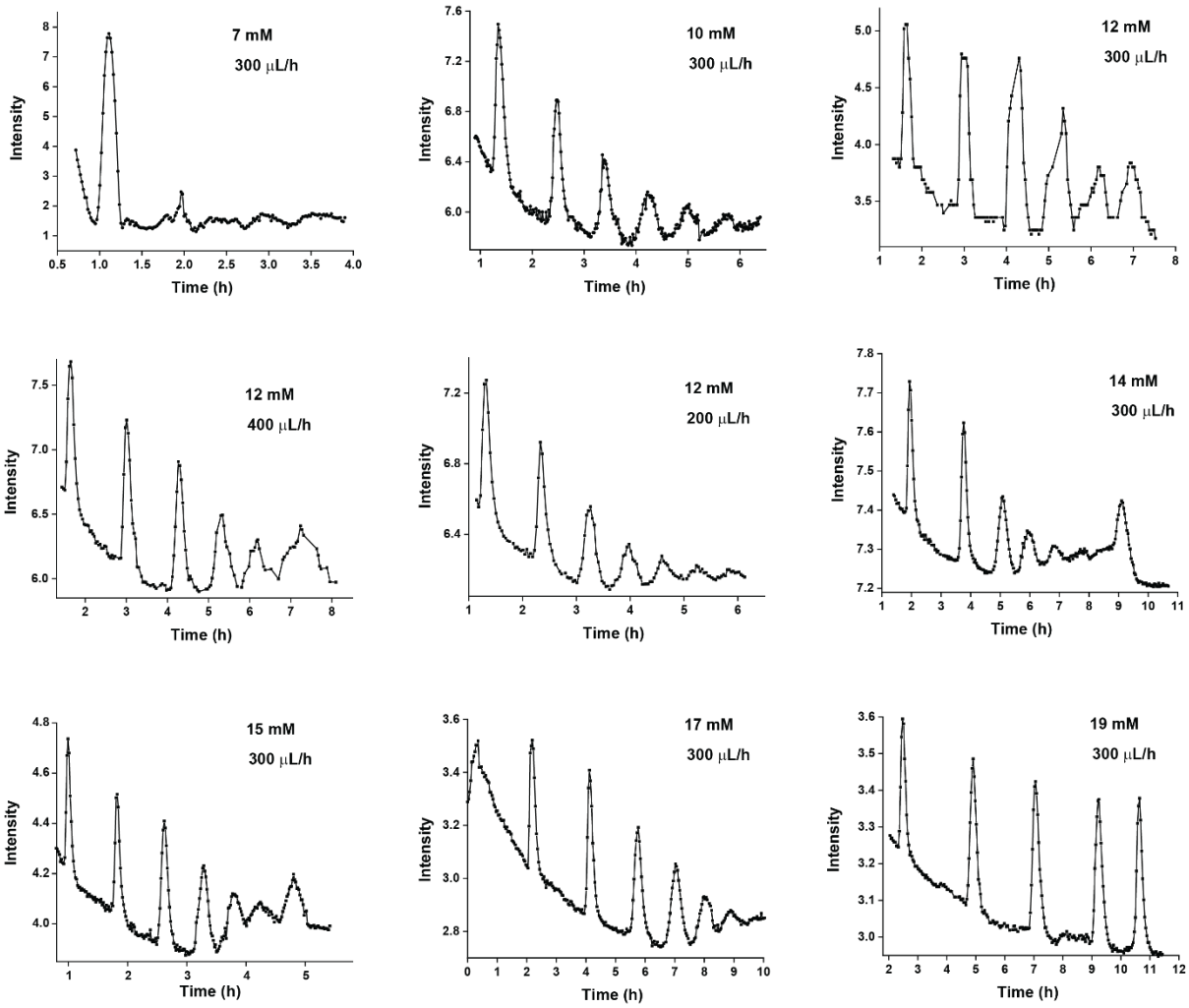

Figure S12. Oscillatory plots from experiments with different amounts of **TPEG-Mal**. The plots were obtained by measuring intensity at a chosen point in the hydrogel (for details, see the data analysis section). The average **TPEG-Mal** concentration between the two channels and the flow rate in the channels are shown in the plots. The average **TPEG-Mal** concentration approximately reflects the concentration of **TPEG-Mal** in the middle of the hydrogel after equilibration. Detailed experimental conditions for the experiments used in this figure can be found in **Table S1** under labels Exp14-18, 20, 21, 24, 25 (order is left to right, top to bottom).

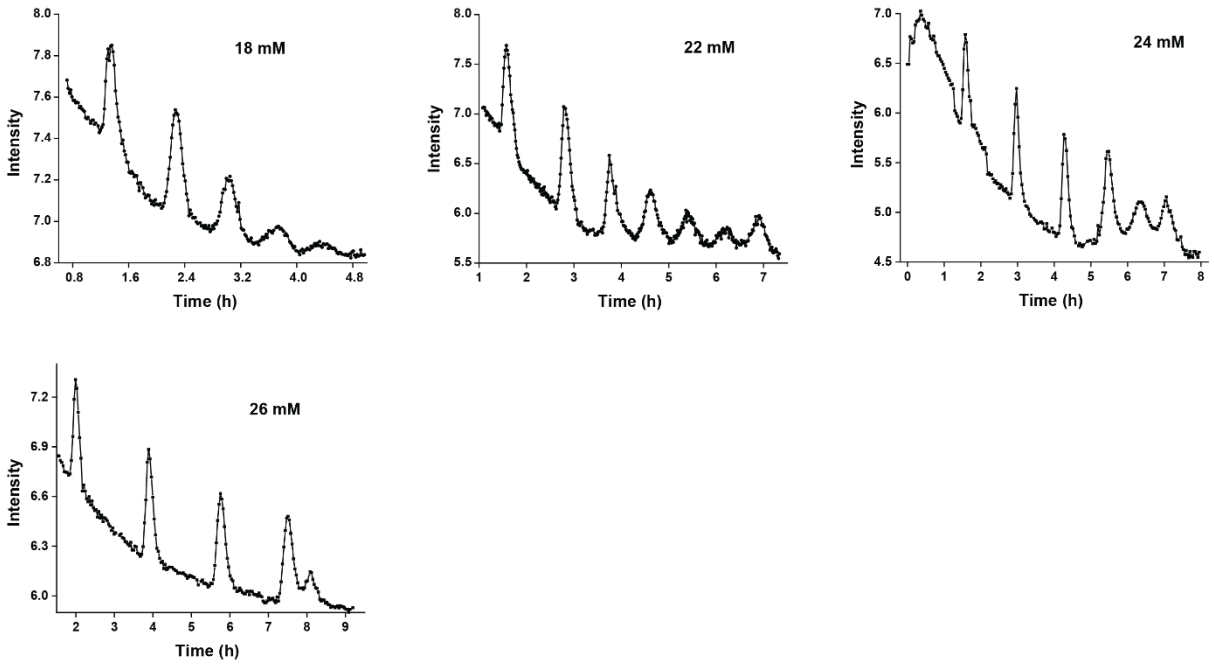

Figure S13. Oscillatory plots from experiments with different amounts of **HPEG-Mal**. The plots were obtained by measuring intensity at a chosen point in the hydrogel (for details, see the data analysis section). The average **HPEG-Mal** concentration between the two channels is shown in the plots. This number approximately reflects the concentration of **HPEG-Mal** in the middle of the hydrogel after equilibration. Detailed experimental conditions for the experiments used in this figure can be found in **Table S1** under labels Exp29-32 (order is left to right, top to bottom).

Determination of diffusion coefficients by DOSY measurements

The ^{1}H Diffusion NMR measurements were performed at 298K on a 9.4T (400.35MHz) AVANCE NEO spectrometer equipped with a 50 gauss/cm Z gradient system. The LED (longitudinal eddy current delay) pulse sequence was used with smoothed square (SMSQ.10.100) gradients. The gradients were incremented from 2% to 98% in 10 linear steps and 8 scans were acquired for each gradient. The gradient duration was 2ms and the diffusion time was 30ms.

The following diffusion coefficients were calculated as an average of 3 consecutive experiments performed for each sample (Table S2):

Compound	Mw [gr/mol]	D [x10^{-5}] cm^2/s
Cystamine (**2**)	154	0.474±0.001
Cysteamine	77	0.695±0.008
Acrylamide (**3**)	71	0.753±0.010

The following diffusion coefficients were calculated as an average of different signals of the same molecule (Table S3):

Compound	Mw [gr/mol]	D [x10^{-5}] cm^2/s
Thiouronium salt (**1**)	163	0.486
Maleimide (**Mal**)	97	0.776
TPEG-Mal	243	0.523±0.002
HPEG-Mal	375	0.302±0.024

Analysis of the waves

Analysis of the intensity at a spot: oscillatory plots. All the image processing and analysis were conducted using ImageJ.exe software. First, all the pictures were stacked in ImageJ to create a stack. If necessary, rotation adjustments were made to align the images properly. The stack was then split into three channels (red, green, and blue). Either the red or green channel was chosen for further analysis, depending on where the contrast was better. A small square area was selected for analysis. For each time point, the mean value of pixel intensities was measured within this square. This intensity was plotted against time to generate graphs that reflect oscillations in thiol concentration at the chosen location caused by the passage of waves.

Analysis of the rates of propagation of waves. First, pictures corresponding to a selected wave were segregated from all the pictures for an experiment. The selected pictures were stacked in ImageJ to create a stack. As before, alignment, channel splitting, and contrast correction were performed. Either the red or green channel was chosen for further analysis depending on where the wave movement was more visible, and colour adjustments were made if necessary. A narrow rectangular area was selected in the middle of the hydrogel where the maximum wave movement was observed. Next, in the analysis section of ImageJ, the "plot profile" function was selected, and live mode was switched on. The middle point of the y-axis [(highest peak - base peak)/2 + base peak] was identified for each time point (profile from an image). The x-axis values corresponding to the y-axis middle points were manually recorded. Finally, these x-axis values were plotted against time to reflect the propagation of the waves. The slope of the linear fit of this plot provides the rate of wave propagation. This procedure needs to be performed separately for each wave in an experiment.

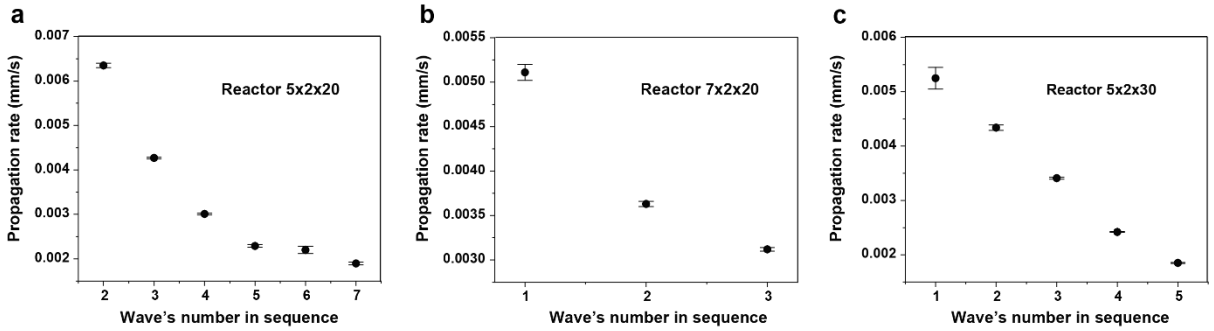

Figure S14. Linear propagation rate of the waves as determined by the rate of movement of the point at half-height from the wave's base to crest for experiments with different reactor geometries. Experimental conditions: 25 °C, right channel – H_2O, [**1**] = 100 mM, [**Mal**] = 4 mM, [**3**] = 800 mM, flow = 200 µL/h, left channel – 2 M Tris-buffer pH 7.5, [**2**] = 200 mM, flow = 200 µL/h. (a) Experiment in the reactor with dimensions 5x2x20mm. (b) Experiment in the reactor with dimensions 7x2x20mm. (c) Experiment in the reactor with dimensions 5x2x30mm.

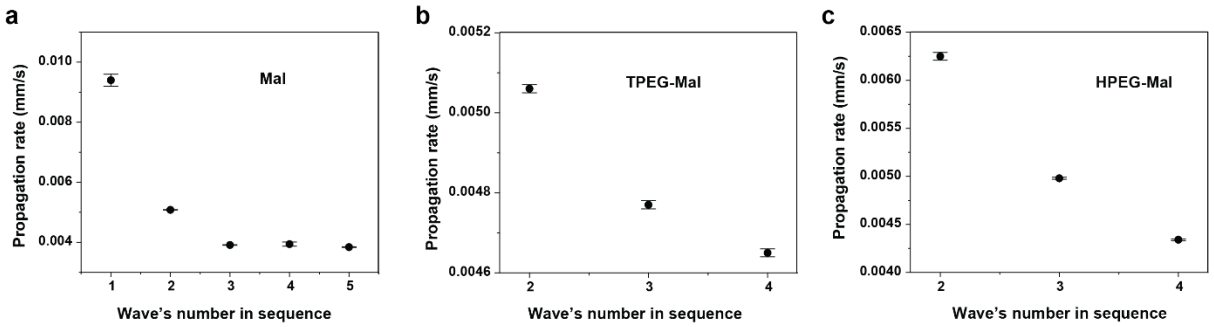

Figure S15. Linear propagation rate of the waves as determined by the rate of movement of the point at half-height from the wave's base to crest for experiments with different derivatives of maleimide. Experimental conditions: 25 °C, right channel (as in the image) – H_2O, [**1**] = 100 mM, [**3**] = 800 mM, flow = 300 µL/h, concentrations of corresponding maleimides are shown in the figure, left channel (as in the image) – 2 M Tris-buffer pH 7.7, [**2**] = 200 mM, flow = 300 µL/h. (a) The experiment with **Mal**. right channel [**Mal**] = 10 mM; left channel [**Mal**] = 4 mM. (b) The experiment with **TPEG-Mal**. right channel [**TPEG-Mal**] = 22.5 mM; left channel [**TPEG-Mal**] = 12.5 mM. (c) The experiment with **HPEG-Mal**. right channel [**HPEG-Mal**] = 35 mM; left channel [**HPEG-Mal**] = 17 mM.

Numerical modeling

The suggested mechanism describing the experimental findings

$$\mathrm{TU} \xrightarrow{k_H} \mathrm{RSH} \quad (1)$$

$$\mathrm{CSSC + RSH} \xrightarrow{k_{SS}} \mathrm{CSH + SS} \quad (2)$$

$$\mathrm{CSH + SS} \xrightarrow{k_{SS}} \mathrm{CSSC + RSH} \quad (3)$$

$$\mathrm{TU + CSH} \xrightarrow{k_L} \mathrm{2\,RSH} \quad (4)$$

$$\mathrm{Mal + RSH} \xrightarrow{k_{Mal}} \emptyset \quad (5)$$

$$\mathrm{Mal + CSH} \xrightarrow{k_{Mal}} \emptyset \quad (6)$$

$$\mathrm{AAm + RSH} \xrightarrow{k_{AAm}} \emptyset \quad (7)$$

$$\mathrm{AAm + CSH} \xrightarrow{k_{AAm}} \emptyset \quad (8)$$

where TU represents thiouronium salt, RSH thiols, CSSC cystamine, CSH cysteamine, SS disulfides, Mal maleimides, and AAm acrylamide.

The spatiotemporal evolution of a compound is determined by the diffusion and the kinetic terms according to the component balance as

$$\frac{\partial c_i}{\partial t} = D_i \nabla^2 c_i + f(c_i), \quad (9)$$

where D_i corresponds to the diffusion coefficient of species i, $f(c_i)$ represents the kinetic term.

The governing equations of the system in the gel are given by the following equations

$$\frac{\partial[\mathrm{TU}]}{\partial t} = D_{\mathrm{TU}}\nabla^2[\mathrm{TU}] - k_H[\mathrm{TU}] - k_L[\mathrm{TU}][\mathrm{CSH}] \quad (10)$$

$$\frac{\partial[\mathrm{RSH}]}{\partial t} = D_{\mathrm{RSH}}\nabla^2[\mathrm{RSH}] + k_H[\mathrm{TU}] - k_{SS}[\mathrm{CSSC}][\mathrm{RSH}] + k_{SS}[\mathrm{CSH}][\mathrm{SS}] + 2k_L[\mathrm{TU}][\mathrm{CSH}] - k_{Mal}[\mathrm{Mal}][\mathrm{RSH}] - k_{AAm}[\mathrm{RSH}][\mathrm{AAm}] \quad (11)$$

$$\frac{\partial[\mathrm{CSSC}]}{\partial t} = D_{\mathrm{CSSC}}\nabla^2[\mathrm{CSSC}] - k_{SS}[\mathrm{CSSC}][\mathrm{RSH}] + k_{SS}[\mathrm{CSH}][\mathrm{SS}] \quad (12)$$

$$\frac{\partial[\mathrm{CSH}]}{\partial t} = D_{\mathrm{CSH}}\nabla^2[\mathrm{CSH}] + k_{SS}[\mathrm{CSSC}][\mathrm{RSH}] - k_{SS}[\mathrm{CSH}][\mathrm{SS}] - k_L[\mathrm{TU}][\mathrm{CSH}] - k_{Mal}[\mathrm{Mal}][\mathrm{CSH}] - k_{AAm}[\mathrm{CSH}][\mathrm{AAm}] \quad (13)$$

$$\frac{\partial[\mathrm{SS}]}{\partial t} = D_{\mathrm{SS}}\nabla^2[\mathrm{SS}] + k_{SS}[\mathrm{CSSC}][\mathrm{RSH}] - k_{SS}[\mathrm{CSH}][\mathrm{SS}] \quad (14)$$

$$\frac{\partial[\mathrm{AAm}]}{\partial t} = D_{\mathrm{AAm}}\nabla^2[\mathrm{AAm}] - k_{AAm}[\mathrm{RSH}][\mathrm{AAm}] - k_{AAm}[\mathrm{CSH}][\mathrm{AAm}] \quad (15)$$

$$\frac{\partial[\mathrm{Mal}]}{\partial t} = D_{\mathrm{Mal}}\nabla^2[\mathrm{Mal}] - k_{Mal}[\mathrm{Mal}][\mathrm{RSH}] - k_{Mal}[\mathrm{Mal}][\mathrm{CSH}] \quad (16)$$

The flow channels are positioned at the left and the right side of the gel where the additional term of $u\nabla c_i$ is added to each component balance to represent the flow. The partial differential equations are first discretized using an equidistant grid with spatial resolution h = 0.004 cm. The diffusion terms are discretized using a 9-point Laplacian and the centred difference formula for the flow term in the

channels. The ordinary differential equations are solved with the Backward differentiation formula utilizing the CVODE package with 10^{-6} relative tolerance in the concentrations. The size of the reactor, containing the gel and the two side channels, was 96 × 501 points matching the experimental interchannel area (3.8 × 20 mm). Within this domain the left and right 10 × 501 points from both sides contain the channels where plug flow is considered with constant fluid velocity parallel to the gel. This approximation basically represents the source and sink for the gel reactor. On the top edge of the channels Dirichlet boundaries were set as an approximation for the in-flow of reactants beacuse reaction rates are neglegible at these locations. No-flux boundaries were set at all other edges of the reactor. No chemicals are initially in the reactor, and four chemicals were flown in the channels, resembling the experimental conditions. The rate coefficients and the diffusion coefficients along with the in-flow concentrations of the reactants and the linear flow rate are summarized in Table S4.

Table S4: Applied parameters

Name/unit	**Symbol**	**Value**	**Unit**
diffusion coefficient of thiols	dRSH	1.44	$mm^2\ h^{-1}$
diffusion coefficient of maleimide	dMal	1.4-2.1	$mm^2\ h^{-1}$
diffusion coefficient of thiouronium salt	dTU	1.512	$mm^2\ h^{-1}$
diffusion coefficient of cystamine	dCSSC	1.44	$mm^2\ h^{-1}$
diffusion coefficient of cysteamine	dCSH	1.44	$mm^2\ h^{-1}$
diffusion coefficient of disulfides	dSS	1.44	$mm^2\ h^{-1}$
diffusion coefficient of acrylamide	dAAm	2.34	$mm^2\ h^{-1}$
rate coefficients of eqn. (1)	k_H	0.1332	h^{-1}
rate coefficients of eqns (2)-(3)	k_{SS}	2400	$dm^3\ mol^{-1}\ h^{-1}$
rate coefficient of eqn. (4)	k_L	4200	$dm^3\ mol^{-1}\ h^{-1}$
rate coefficients of eqns (5)-(6)	k_{Mal}	5.4×10^5	$dm^3\ mol^{-1}\ h^{-1}$
rate coefficients of eqns (7)-(8)	k_{AAm}	100	$dm^3\ mol^{-1}\ h^{-1}$
in-flow concentration of maleimide (left channel)	Mal0L	6.0-12.5	$mmol\ dm^{-3}$
in-flow concentration of maleimide (right channel)	Mal0R	2.4-5.0	$mmol\ dm^{-3}$
ratio of the in-flow concentration of maleimide (left/right channel)	R	2.5	
in-flow concentration of thiouronium salt (left channel)	TU0	0.1	$mol\ dm^{-3}$
in-flow concentration of cystamine (left channel)	CSSC0	0.4	$mol\ dm^{-3}$
in-flow concentration of acrylamide (right channel)	AAm0	0.8	$mol\ dm^{-3}$
linear flow rate	u	14-30	$cm\ h^{-1}$

Machine learning

First, using a uniform sampling of parameter values in a region of interest, we ran 25 simulations of the numerical model and then used a convolutional autoencoder on the individual frames of the simulation to reduce the 7 spatial concentration profiles to a latent space of 500 variables. The autoencoder was able to accurately reconstruct the original frames, indicating that the latent space is able to fully capture the details of the system. We then trained a recurrent neural net to map from sequences of points in the latent space to the input parameter space varying D_I (diffusion coefficient of maleimide) and I_0 (concentration of maleimide supplied to the gel). To predict the phase boundary, we used a linear SVM classifier to find the boundaries between different behaviors. We then used the parameter map we had previously trained to project the boundary into the parameter space (Fig. S16). These boundaries are hyperplanes in the latent space, and trajectories on the hyperplane need to be sampled to project back to the parameter space. To achieve we took the closest point on the hyperplane to each existing point from the frames of the original simulations. The parameter map is the most accurate at estimating points close to parameter combinations it was trained on, so if a point is projected to the hyperplane from too far away it can move into regions of the latent space the parameter estimator hasn't seen, leading us to estimate the phase boundary using only points close enough to the hyperplane. The estimated boundary is very sensitive to the choice of distance cutoff, but there are a few metrics that can be considered based on characteristics of the data and the shape of the boundary. Distance from the separating hyperplane can be used as a predictive metric for behavior.[5, 6]

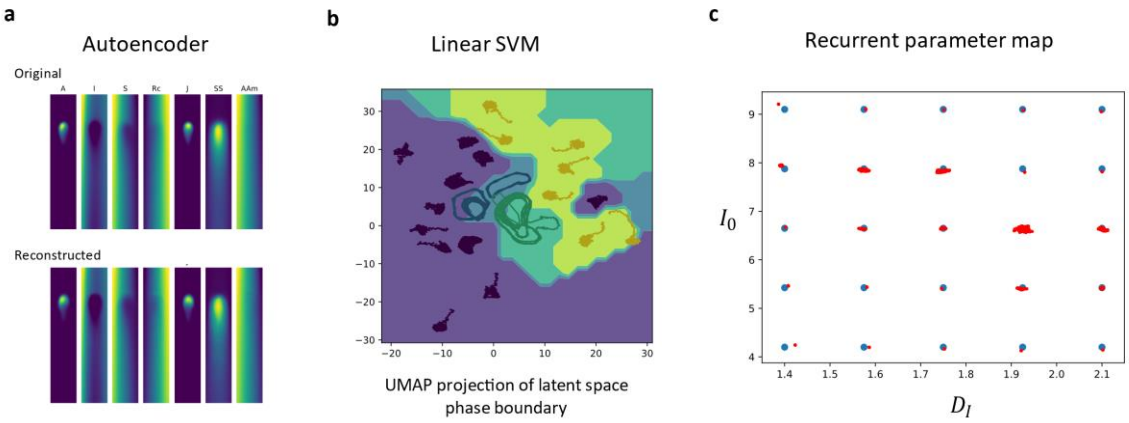

Figure S16. Learning tasks for phase boundary estimation. (a) The autoencoder learns the minimal space of frames. (b) Linear SVM learns separating hyperplanes between labeled points in latent space. (c) Train recurrent neural network on trajectories in latent space to estimate input parameters. The parameter map is less accurate for more oscillatory results as well as points far from existing parameter combinations.

Once the boundary is predicted we can refine it using a small number of resampled points to update the parameter estimator and SVM boundary to converge on an estimated phase boundary quite quickly (Fig.

S17). The improvement of the boundary is not sensitive to the exact choice of resampled points as long as they cover an area near the boundary, preferably spaced away from existing points to aid the parameter estimator.

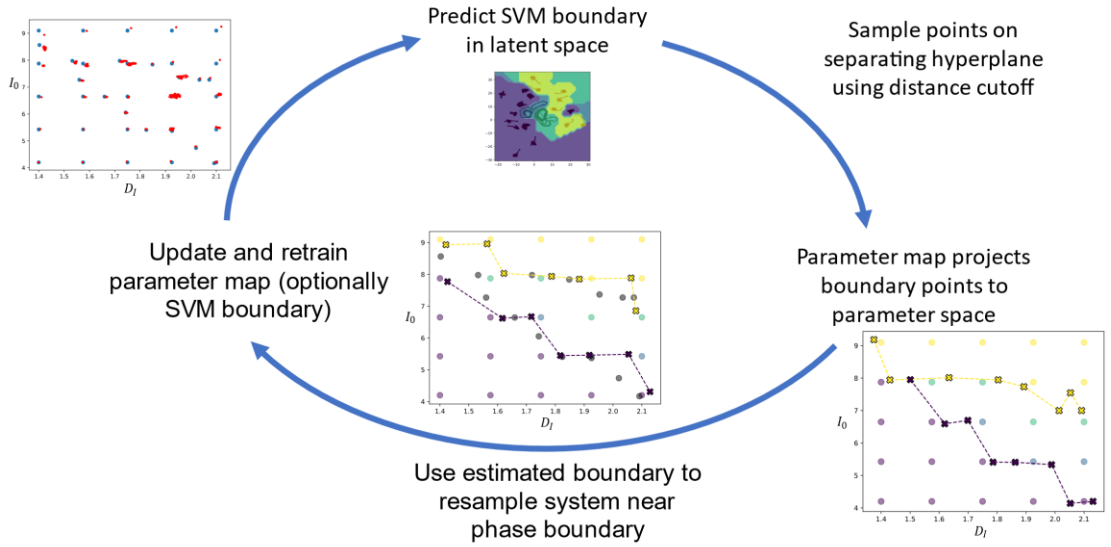

Figure S17. Phase boundary estimation iteration loop.

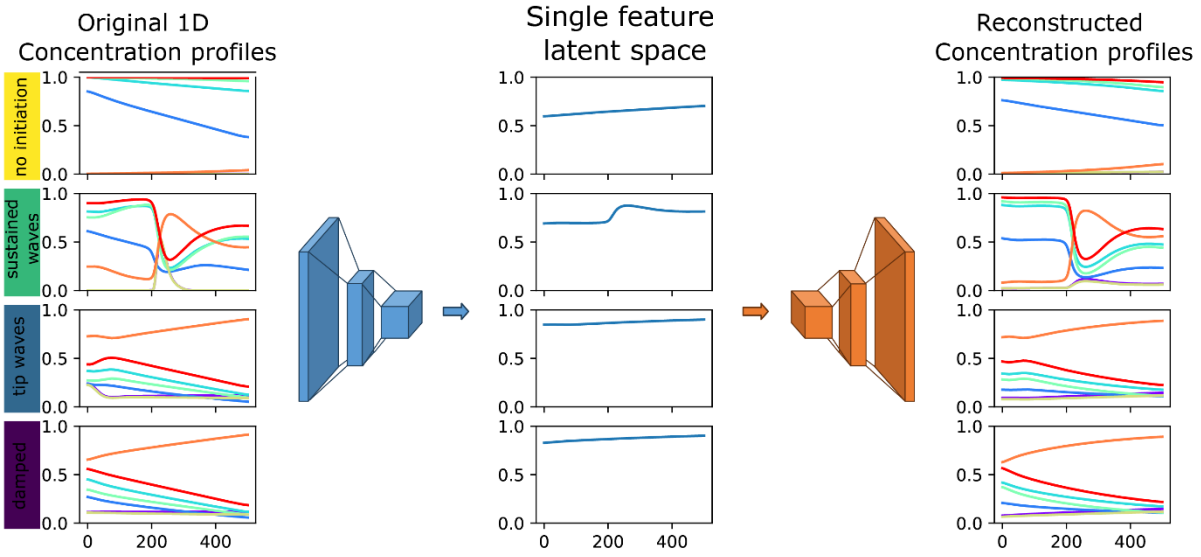

Figure S18. For each space and time point the autoencoder learns a single latent variable from the seven simulated chemical channels. This allows us to capture wave propagation dynamics of the wave pulse as a whole as opposed to the evolution of a single species. Even a single latent variable can reconstruct the original data fairly wellю

References

1. A. I. Novichkov, A. I. Hanopolskyi, X. Miao, L. J. W. Shimon, Y. Diskin-Posner and S. N. Semenov, *Nat. Commun.*, 2021, **12**, 2994.
2. K. Umezawa, M. Yoshida, M. Kamiya, T. Yamasoba and Y. Urano, *Nat. Chem.*, 2017, **9**, 279-286.
3. C. Hammaecher, B. Joris, E. Goormaghtigh and J. Marchand-Brynaert, *Eur. J. Org. Chem.*, 2013, **2013**, 7952-7959.
4. D. C. Duffy, J. C. McDonald, O. J. A. Schueller and G. M. Whitesides, *Anal. Chem.*, 1998, **70**, 4974-4984.
5. E. D. Cubuk, S. S. Schoenholz, E. Kaxiras and A. J. Liu, *J. Phys. Chem. B*, 2016, **120**, 6139-6146.
6. S. S. Schoenholz, E. D. Cubuk, D. M. Sussman, E. Kaxiras and A. J. Liu, *Nat. Phys.*, 2016, **12**, 469-471.